Energy, Volume 201, June 2020, Article number 117597
DOI: 10.1016/j.energy.2020.117597

Performance analysis of a novel combined solar trough and tower aided coal-fired power generation system

Hongtao Liu[a,b], Rongrong Zhai[a,*], Kumar Patchigolla[b], Peter Turner[b], Yongping Yang[a]

[a] Key Laboratory of Condition Monitoring and Control for Power Plant Equipment, Ministry of Education, North China Electric Power University, Beijing 102206, China

[b] School of Water, Energy and Environment, Cranfield University, Bedfordshire MK43 0AL, UK

*Corresponding author: Rongrong Zhai

E-mail: zhairongrong01@163.com

Abstract: Solar-aided coal-fired power generation systems have been extensively studied and exhibit several advantages in the utilisation of solar energy. The issue with the solar augmentation of coal-fired plants is the limitation of the potential solar contribution that it is practical to achieve considering the thermal balance and boiler safety issues. This study proposes the original combined parabolic troughs and solar towers to collect solar energy, and then introduce it into preheaters and boilers in coal-fired power plants. Under the same investment condition, the combined solar field can collect more solar exergy and obtain improved constrains for the solar energy contribution. The simulation results of the combined solar field integrated with a 660MW_e power plant show a highest solar exergy share of 8.45% is reached, leading to at least 1.58 and 4.24 g/kWh coal fuel further saving compared to other two systems under a nominally similar investment for the solar field, which gives a minimum of 253.17 and 255.83 g/kWh, respectively. The maximum available solar exergy is 69.43 MW_{th}, which is 7.83%–11.88% higher than compared systems. The enhanced solar

exergy contribution and cost-effectiveness can be also approached in this novel system under different solar load and cost conditions.

Keywords: Solar-aided coal-fired power generation system; parabolic trough; solar tower; solar exergy share; available solar exergy

1 Introduction

With the rapid global economic development, energy plays an irreplaceable role, and fossil fuels continue to dominate the world energy system, with coal-fired power generation as the main source [1]. In 2017, global fossil fuel power generation accounted for 64.7%, of which 58.9% (9723.4 TWh) came from coal-fired power generation [2]. However, coal-fired power plants are under immense pressure of numerous environmental problems. Increasing the use of renewable energy is urgently needed [3].

Compared with other renewable energy sources, such as wind and photovoltaic energy, concentrating solar power (CSP) has the key advantage that, combined with thermal energy (heat) storage (TES), it can provide stable and dispatchable electricity [4]. On the other hand, the stand-alone CSP system also has obstacles including high investment and large-scale TES or fuel-based backup power requirement. Integrating

solar thermal energy with coal-fired power plants, namely, solar-aided coal-fired power generation, is an effective way to reduce coal consumption in coal-fired power plant, decrease carbon dioxide emissions, and reduce initial investment by sharing virtually all the power block components. Many scholars have conducted studies on solar parabolic trough aided coal-fired power generation (SPCG) and solar tower aided coal-fired power generation (STCG) systems.

Zoschak and Wu were the first to propose the integration of solar and coal-fired power generation in 1975 [5]. They introduced solar thermal energy into an 800 MW_e fossil-fuel steam power plant in seven different schemes and qualitatively compared the performances. Results showed that the combined evaporation and superheating proved to be the preferred method because of high utilisation of solar energy and relatively low capital cost. Hu and Yang then proposed the solar-aided coal-fired power generation concept using solar heating at a relatively low-temperature range (up to 350 °C) in a traditional regenerative Rankine cycle [6]. Yang et al. indicated that with the same temperature level of solar input, the integrated system can reach a higher solar-thermal-to-electricity conversion efficiency than a solar alone power plant because of higher steam temperatures and pressures [7]. Later the same group investigated several different schemes in power-boosting and fuel-saving modes based on a 200 MW_e coal-fired power generation system [8, 9].

On this basis, many researchers have conducted studies on the SPCG system. Rech et al. compared 20 different integration schemes in a 320 MW_e SPCG considering the technical constraints related to the maximum and minimum loads of all components;

the optimal integration point also results in high-pressure preheaters, with the highest hybrid thermal efficiency of 42.67% and solar share of up to 9.1% [10]. The topology structure and control strategy are also considered to find the optimal integration scheme [11]. Li et al. analysed the safe operation limitation of a 600 MW_e SPCG system in Simulink. The simulation results showed that the maximum introduced solar energy is 66.5 MW_{th} considering the operational safety of the boiler [12]. Wu et al. studied the influence of introduced solar power on mass-flow rate and temperature variation of superheated and reheated steam [13]. They suggested that replacing the extraction steam in the third stage would not affect the temperature of the main or reheated steam [14]. Then the annual performance study showed the minimum levelized energy cost of \$0.06/kWh is obtained [15]. The influence of parameters, including TES hours, solar multiple, and the ratio of row spacing to aperture width, on the annual economic performance are also studied [16].

Hou et al. investigated the performance of the SPCG system under off-design conditions and found that solar-to-electricity efficiency varies between 8.09% and 26.16% in part load condition [17]. Peng et al. investigated hourly thermodynamic performances on typical days and obtained a similar conclusion [18]. Zhang et al. observed the transient performance in a typical solar irradiation system [19]. Wang et al. developed a general system integration optimisation model that uses eight virtual heat exchangers to simulate all schemes integrated into the regenerative system, with different integration positions and thermal load distributions [20]. The multi-objective optimisation was performed to consider off-design conditions [21].

The performance of key units in the SPCG systems is also a concern in recent years. Feng et al. applied a flash tank to avoid the unstable two-phase flow problem in solar collector tubes, improving the feasibility of system implementation [22]. Considering the shortage of cooling water supply in most solar-rich areas, Huang et al. investigated the performance of SPCG systems configured with a direct air-cool condenser and proposed four operating strategies of the air-cool condenser [23]. They also proposed a method of adjusting the burner tilt to 22.7° and attemperation flows in boiler to maintain the temperature of superheated and reheated steam at 543 °C [24].

The evaluation of the SPCG system was also explored. Zhai et al. proposed the amount of coal saving in unit solar investment as an evaluation function and optimized the integrated solar collector area [25]. Thermo-economic structural theory was then applied to compare the performance of this system in fuel-saving and power-boosting modes [26]. Zhu et al. compared five common solar contribution evaluation methods in 1000, 600, and 330 MW_e SPCG plants [27]. Suresh et al. undertook a 4-E (energy, exergy, environment, and economic) analysis on 500 and 660 MW_e supercritical coal-fired power plants in India [28]. The comparison between SPCG power and the stand-alone CSP plants was performed by Pierce et al. by using weather data from Lephalale, South Africa [29]. The annual power generation from solar energy in the former was more than 25% higher than that of the latter. With regard to cost reduction due to the shared power equipment, solar subsystem in SPCG is 1.8 times more cost-effective than that of an independent CSP. Jamel et al. summarised the integration technology of SPCG systems and suggested considerable advantages for this technology, especially

for existing power plants [30].

Compared with parabolic trough collectors, the higher concentration factor of a solar tower means it is possible to extract solar energy at a high temperature, leading to higher solar-to-electricity efficiency. Therefore, the integration based on solar tower and boilers has been emphasized. An advanced exergy analysis on a 1000 MW_e STCG system was conducted to explore the exergy destruction [31]. Results showed that endogenous exergy destruction accounts for more than 70% of exergy destruction, and the connection of the solar tower and boiler is feasible. The study of the annual performance indicates that the solar-to-electricity exergy efficiency of this system increased by at least 1.83 % compared with that of stand-alone solar power plant due to the better steam conditions and a larger plant capacity [32]. Then the economic analysis demonstrated that the project exhibited high profits with an internal rate of return of 8.70% [33]. Zhang et al. used solar energy to heat superheated steam or sub-cooled feed-water in a practical 660 MW_e supercritical power plant [34]. The standard coal consumption could decrease by more than 17 g/kWh (5.40%). The maximum solar shares in two schemes are 6.11% and 4.90% due to the thermal balance limitation of boiler. The off-design performance showed that the solar-to-electricity conversion efficiency varies in the range of 16.7%–19.6% [35]. Li et al. compared three different schemes for integrating solar thermal energy into boilers under fuel-saving and power-boosting modes [36]. Using solar energy to heat superheated steam and sub-cooled feed-water tends to have optimal performance, saving 11.15 and 11.11 g/kWh coal consumption rates in the two operating modes. Then the performances at 100%, 75%,

and 50% loads showed that 76.4, 54.2, and 23.0 MW_{th} solar power can be introduced into the system under three off-design conditions [37]. The annual system performance considering variable load demand was then investigated [38].

These studies have conducted detailed investigations on the system simulation, operation performance, and evaluation of the SPCG and STCG systems. However, in these works, only the stand-alone parabolic troughs or tower is focused on, leading to a limited solar thermal energy contribution considering the safety limitations of the boiler and the need for a constant temperature of superheated steam and reheat steam. Moreover, parabolic trough collectors and solar tower have complementary characteristics in collecting heat, that can be combined for better efficiency and economy. The novelty of the present work is to propose an original integration of coal-fired power plant with a combined solar field composed of parabolic trough collectors and solar tower (PTCG) to improve the solar contribution limitation and explore solar field configuration with higher cost-effectiveness. In this study, four different schemes of PTCG system under different investment distribution between solar trough and tower are studied and compared with other systems in previous studies at design point. The effects of solar conditions, total investment, and solar field cost are investigated.

2 System description

2.1 PTCG system

Four different schemes of PTCG systems are displayed in Figures 1 and 2. This integrated system is composed of solar field components and conventional coal-fired

power plant. The solar field includes heliostat field, solar tower, receiver, trough collectors, TES system, and heat exchangers. In the heliostat field, solar energy is reflected by heliostats to the receiver on the top of the tower. Molten salt is pumped through the receiver and heated up to a practical maximum of 600 ℃. The thermal energy of hot salt is released in heat exchangers and transferred to the steam cycle. The molten salt used in this study is the solar salt (wt. 60% $NaNO_3$+40% KNO_3). In the parabolic trough collector field, solar energy is reflected from the parabolic trough to the vacuum tube. The heat transfer fluid (HTF) is pumped through the collector and heated. The thermal energy of HTF is released and transferred to the steam cycle in a heat exchanger.

The original coal-fired power unit is a practical 660 MW_e supercritical steam unit, single intermediate reheat, including a boiler, steam turbine, generator, condenser, deaerator, and feed-water heaters. The regenerative system comprises three high-pressure reheaters (PH1, PH2, and PH3), four low-pressure reheaters (PH5, PH6, PH7, and PH8), and a deaerator.

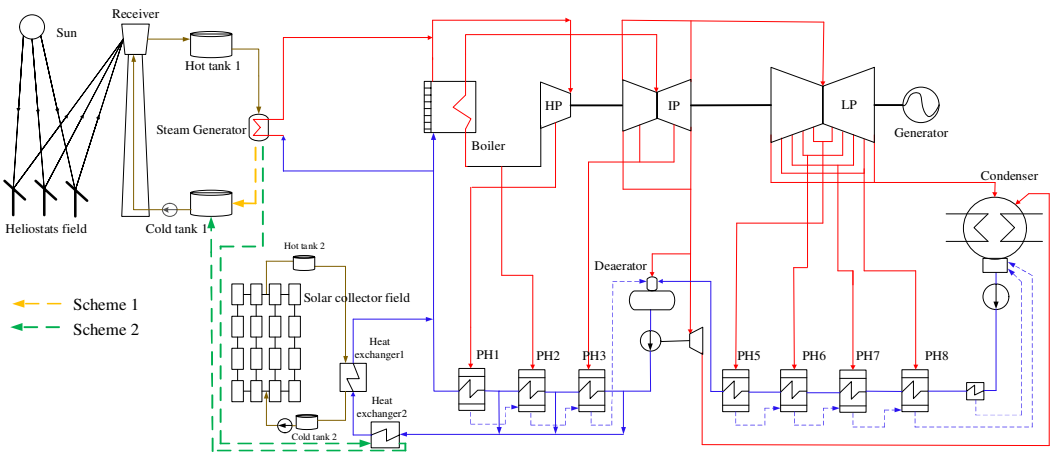

Figure 1. Diagram of the PTCG system in schemes 1 and 2

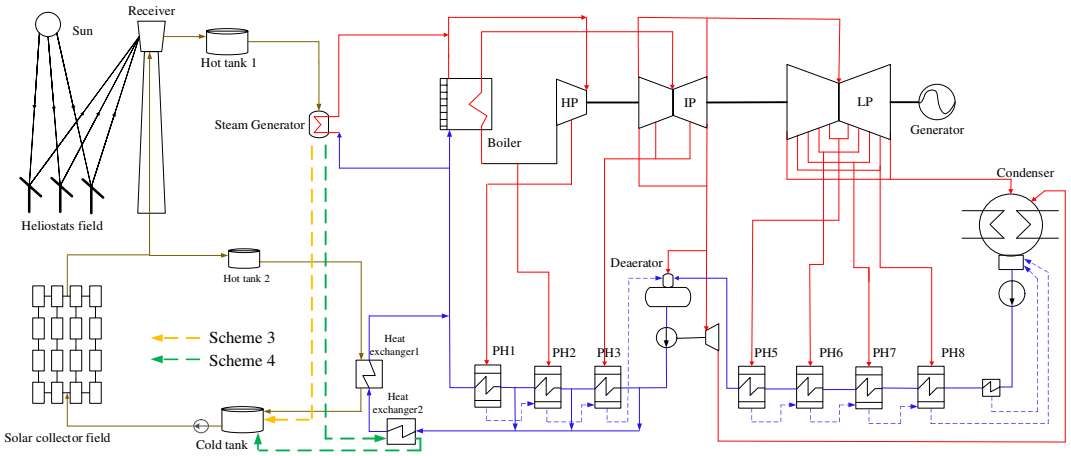

Figure 2. Diagram of the PTCG system in schemes 3 and 4

2.2 Integration schemes

In scheme 1, the solar thermal energy from the solar tower field is used to partly replace thermal load of economizer, water wall, and super-heater in the boiler to produce superheated steam. The outlet temperature of superheated steam is 566 °C. The flow rate of extracted feed-water from the boiler inlet depends on the available solar thermal energy and safe operation restriction of boilers. The solar thermal energy from the collector field is used to partly replace the steam extraction to heat feed-water. In scheme 2, the molten salt from the steam generator is then used to preheat the feed-water in heat exchanger 2 before returning to the cold tank. The solar thermal from solar trough is still used to heat feed-water in heat exchanger 1.

In scheme 3, the trough collectors and the receiver are connected in series to collect solar thermal energy. Molten salt is pumped through the collector field to absorb thermal energy, and then sent into the receiver. To ensure the molten salt at the receiver outlet can be heated to 580 °C, part of the molten salt at the collector field outlet is extracted to heat the feed-water in exchanger 1 to control the mass-flow of molten salt

that sent into the receiver. In this way, the molten salt temperature at outlets of collector field and receiver can be consistent under different sizes of collector field and heliostat field. In scheme 4, trough collectors and the heliostat field are also connected in series to collect solar thermal energy. Different with scheme 3, molten salt from the steam generator is used to preheat the feed-water in heat exchanger 2 before returning to the cold tank.

The extraction of feed-water at the boiler inlet and partial replacement of the thermal load of economizer, water wall, and super-heater will affect the thermal balance inside the boiler and lead to safety issue. Zhang et al. reported that the maximum feed-water extraction mass-flow from the boiler inlet in a 660 MW_e power plant is 8% to maintain the temperature of superheat steam and reheat steam [34]. Therefore, the maximum extraction at the boiler inlet is assumed as 8% mass-flow rate (40.81 kg/s), meaning that maximum 89.56 MW_{th} solar thermal energy can be introduced into the boiler. For constrains for energy from trough collectors, at most 3 stages of high-pressure extracted steam can be replaced to maintain the structure of original power plant, and feed-water temperature at the boiler inlet is kept constant.

3. Thermal performance evaluation criteria

Coal consumption rate is calculated to directly evaluate the system performance:

$$b = \frac{3.6\times10^6 E_{coal}}{LHV\cdot P_e} \quad (1)$$

where E_{coal} is the thermal energy required from coal fuel, MW; LHV is the low heating value of coal fuel, 29310 kJ/kg; P_e is the power output from the system, MW.

Solar energy share (λ_{en}) and solar exergy share (λ_{ex}) are calculated to present the

contribution proportion of solar energy and exergy:

$$\lambda_{en} = \frac{E_{solar}}{E_{coal}+E_{solar}} \tag{2}$$

$$\lambda_{ex} = \frac{Ex_{solar}}{Ex_{coal}+Ex_{solar}} \tag{3}$$

Where E_{solar} and Ex_{solar} are the thermal energy and exergy from solar field, MW; Ex_{coal} is the exergy from coal fuel, MW.

In the situation that maximum mass-flow of feed-water extraction at the boiler inlet or feedwater is reached, thermal energy cannot be further introduced into feed-water and steam, then extra solar energy is stored in the TES. Thus, with the enlargement of the solar field, the solar energy and exergy share are kept unchanged within the plant limitations while available exergy for the system increases. The total available solar exergy is calculated to present the total available solar exergy for system including the exergy introduced into water-steam cycle and the part to be stored:

$$Ex_{total} = Ex_t \cdot \frac{m_{in1}}{m_{out1}} + Ex_p \cdot \frac{m_{in2}}{m_{out2}} \tag{4}$$

Where Ex_t is the exergy introduced into feed-water and steam in steam generator and heat exchanger 2, kJ/kg; m_{in1} and m_{out1} are the mass-flow rate of molten salt from receiver into hot tank 1 and that from hot tank 1 to steam generator, respectively, kg/s; Ex_p is the exergy introduced into feed-water in heat exchanger 1, kJ/kg; m_{in2} and m_{out2} are the mass-flow rate of HTF from collector field into hot tank 2 and that from hot tank 2 to heat exchanger 1, respectively, kg/s.

4 Case studies

4.1 Basic data and model validation

For solar field part, the mathematical model is described and established in MATLAB software in our previous studies [37, 38]. The solar noon on the vernal equinox (21st March) in Delingha (97.37°E, 37.37°N) is selected as design point. The DNI value is set as 800 (W/m^2), the annual average ambient temperature is 4.4 °C, and the annual average wind speed is 2 m/s [39]. The parameters of heliostat from Gemasolar plant and the LS-2 collector are used in this study. The size of heliostat is 12.305 m × 9.752 m. The aperture width of one collector unit is 5.77 m, and the length of each collector unit is 576 m, with the module length of 12 m [26]. The calculation of the heliostat field and receiver has been validated in our previous studies [40, 41].

In this study, the cost of the heliostats is 200 $\$/m^2$ and that of the receiver is 200 \$/kW [42]. The cost of the collector field is 170 $\$/m^2$ [43]. The total solar field investment is 68.27 M\$, which can be used for a stand-alone heliostat field with 2000 heliostats (tower and receiver), or a stand-alone parabolic trough collector field with aperture area of 402.15×10^3 m^2. The nominal power of the solar tower and parabolic trough collector field will change with different investment distributions. The working fluid used in the four schemes and the controlled temperatures are listed in Table 1.

Table 1. Working fluids and temperatures in four schemes

	Scheme 1	Scheme 2	Scheme 3	Scheme 4
HTF in collectors	Thermal oil	Thermal oil	Molten salt	Molten salt
HTF in receiver	Molten salt	Molten salt	Molten salt	Molten salt
Inlet temperature of collectors (°C)	290	290	310	290
Outlet temperature of collectors (°C)	350	350	350	350
Inlet temperature of receiver (°C)	310	290	350	350
Outlet temperature of receiver (°C)	580	580	580	580

A 660 MW_e coal-fired power plant is selected as the basic system, which is an

existing plant in China. The main parameters of the original coal-fired power plant are shown in Table 2.

Table 2. Main parameters of the 660 MW coal-fired power plant

Parameter	PH1	PH2	PH3	Deaerator	PH5	PH6	PH7	PH8
Extraction steam mass-flow rate (kg/s)	26.27	44.84	18.90	25.55	27.51	14.81	14.70	12.75
Extraction pressure (MPa)	5.77	4.23	1.96	1.01	0.41	0.11	0.05	0.02
Extraction specific enthalpy (kJ/kg)	3052.3	2983.1	3379.5	3191.9	2973.4	2718.7	2585.7	2452.9
Drain water temperature (°C)	273.0	253.6	211.2	-	144.1	102.9	80.12	56.84

The calculation of this supercritical coal-fired power plant is performed using Ebsilon Professional. The comparison between the design and calculated value is displayed in Table 3. The table shows that the simulation value is highly consistent with the design value.

Table 3. Comparison of design and simulation values

Parameter	Unit	Design value	Simulation value	Relative error
Power output	MW_e	660	660.67	0.10%
Main steam temperature	°C	566	566	0
Main steam specific enthalpy	kJ/kg	3396.0	3398.8	0.08%
Main steam mass-flow rate	kg/s	510.13	510.13	0
Reheat steam temperature	°C	566	566	0
Reheat steam enthalpy	kJ/kg	3595.7	3597.54	0.05%
Feed-water temperature	°C	274.70	274.73	0.01%
Feed-water enthalpy	kJ/kg	1204.0	1204.38	0.03%
Heat consumption	kJ/kWh	7540.0	7539.12	0.01%

4.2 Results and discussion

At the baseline of the same total investment for solar field, the cost and area of the collectors will increase with the size decrease in heliostat field. The variation of area,

efficiency, and cost of heliostat and collector fields are listed in Table 4. When all investments are used for heliostat field, the system becomes a STCG. When all the investments are used for parabolic collector field, the system becomes a SPCG.

Table 4. Variation of cost distribution and size of solar field

Number of heliostats	Heliostat field efficiency (%)	Gross aperture area of troughs ($\times 10^3$ m^2)	Nominal power of troughs (MW)	Heliostat field investment (M$)	Nominal power of receiver (MW_{th})	Receiver investment (M$)	Collector field investment (M$)
2000	64.32	0	13.59	48.00	101.36	20.27	0.00
1800	65.49	36.56	27.32	43.20	92.89	18.58	6.50
1600	66.69	76.44	41.17	38.40	84.08	16.82	13.06
1400	67.97	116.32	55.12	33.60	74.98	15.00	19.68
1200	69.44	156.21	69.18	28.80	65.66	13.13	26.34
1000	71.16	196.09	83.48	24.00	56.07	11.21	33.06
800	72.79	235.97	98.03	19.20	45.88	9.18	39.90
600	74.28	275.85	112.79	14.40	35.12	7.02	46.85
400	75.71	315.73	127.71	9.60	23.86	4.77	53.90
200	77.50	358.94	142.86	4.80	12.21	2.44	61.03
0	-	402.15	13.59	0.00	0.00	0.00	68.27

Table 5 lists the operation performance of the PTCG system in four schemes in different distributions of solar field investment. With the decrease in size of the heliostat field and more trough collectors arranged, the share of solar thermal energy continues to increase because trough collectors are more cost-effective to collect solar thermal energy, while the share of solar exergy first increases and then decreases, indicating the trough collectors are more cost-effective to collect solar exergy than replaced heliostats at first, and then the efficiency of replaced heliostats increased. The maximum shares of solar energy (9.89%) and exergy (8.45%) can be obtained in scheme 4.

Table 5. Performance of the PTCG system in four schemes

Heliostats Number	Efficiency of heliostat field & receiver (%)	Share of solar energy (%)	Share of solar exergy (%)	Efficiency of heliostat field & receiver (%)	Share of solar energy (%)	Share of solar exergy (%)
	Scheme 1			Scheme 2		
2000	57.95	6.47	6.47	58.04	6.94	6.81
1800	59.01	7.37	7.17	59.10	7.83	7.56
1600	60.18	8.26	7.92	60.27	8.26	7.85
1400	61.27	8.54	8.04	61.37	8.54	7.98
1200	62.55	8.80	8.15	62.65	8.80	8.09
1000	64.11	9.04	8.22	64.21	9.04	8.16
800	65.53	9.23	8.23	65.64	9.23	8.18
600	67.09	9.39	8.19	67.19	9.39	8.15
400	68.20	9.49	8.09	68.31	9.49	8.06
200	69.05	9.64	8.01	69.20	9.64	7.99
0	-	9.77	7.89	-	9.77	7.89
	Scheme 3			Scheme 4		
2000	57.95	6.47	6.42	58.04	6.94	6.81
1800	58.86	6.47	6.42	58.94	6.94	6.81
1600	60.00	7.32	7.14	60.00	7.26	7.08
1400	61.08	8.44	8.08	61.08	8.44	8.07
1200	62.36	8.87	8.33	62.36	8.88	8.34
1000	63.90	9.14	8.42	63.90	9.15	8.43
800	65.32	9.36	8.44	65.32	9.37	8.45
600	66.89	9.55	8.41	66.89	9.57	8.42
400	67.99	9.68	8.30	67.99	9.70	8.32
200	68.75	9.86	8.21	68.75	9.89	8.23
0	-	9.77	7.89	-	9.77	7.89

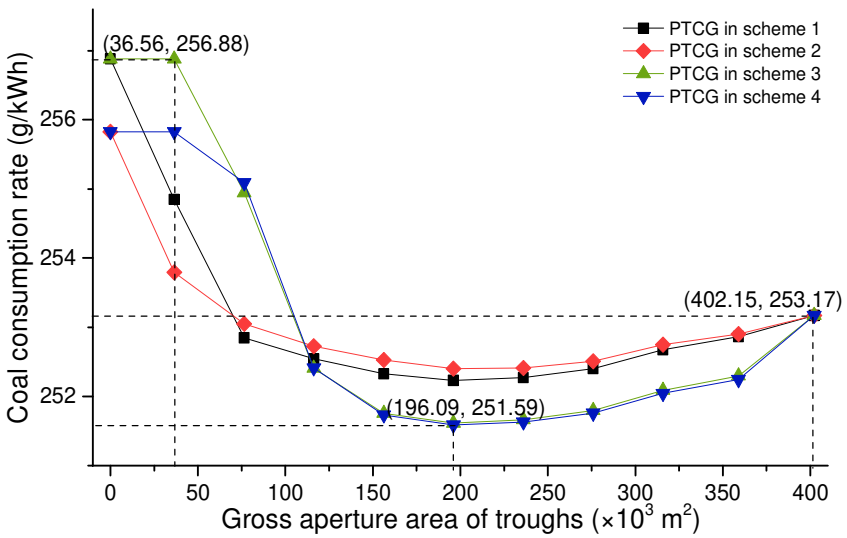

Figure 3. Coal consumption rate in four schemes of the PTCG system

The coal consumption rates in the four schemes of PTCG systems comprising combined solar fields with different investment distributions are shown in Figure 3. The figure illustrates that the coal consumption rate tends to first decrease and then increase with the enlargement of the collector field while maintaining the same solar field investment, which is negatively correlated with the share trend of solar exergy. The figure also demonstrates that all schemes can reach a lower coal consumption rate than that of the SPCG and STCG systems because of an improved solar exergy share. The lowest coal consumption rates in the four schemes are 252.23, 252.40, 251.61, and 251.59 g/kWh, which are 255.80 and 253.17 g/kWh in the STCG and trough SPCG systems, respectively. Moreover, the improved solar share limitation enables more solar exergy to be utilized directly in the system instead of being stored and this reduces the demand for TES capacity. In schemes 1 or 3 with more than 1800 heliostats and schemes 2 or 4 with more than 1400 heliostat, maximum feed-water extraction from the boiler inlet is reached, and the extra energy is stored. In this situation, analysis of total solar exergy available is performed.

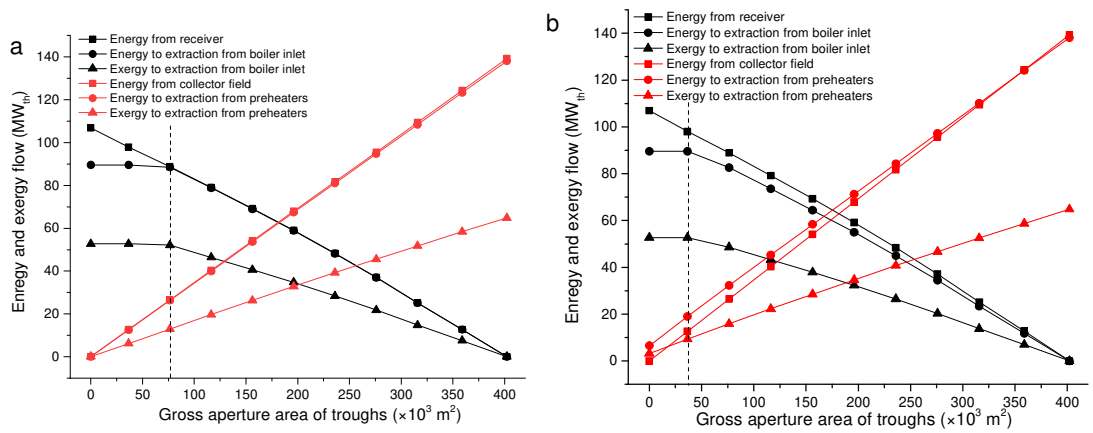

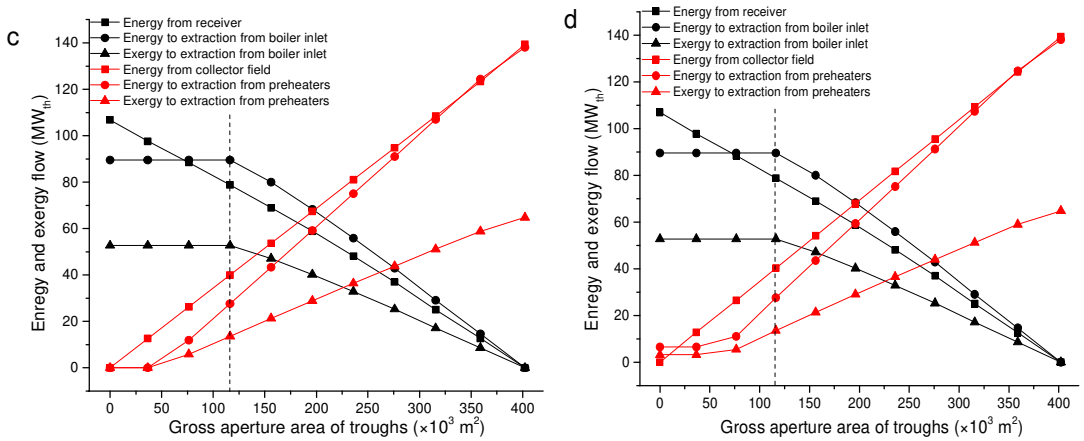

Figure 4. Solar energy and exergy flow under different investment distribution, (a) in scheme 1, (b) in scheme 2, (c) in scheme 3, (d) in scheme 4

The analysis of solar energy and exergy flow in four schemes under different investment distribution are shown in Figure 4. In scheme 1, the solar energy and exergy absorbed in preheating increase to 138.10 and 64.80 MW_e, respectively. In the systems with more than 1600 heliostats, the maximum of feed-water extraction mass-flow from the boiler inlet can be reached and excess energy from solar tower is stored. In scheme 2, the solar energy and exergy absorbed in preheating are 6.52 and 3.21 MW_{th} in the system with no arranged collectors. The feed-water extraction from the boiler inlet is less than 40.81 kg/s in the systems with less than 1800 heliostats. In scheme 3 and scheme 4, in the systems with more than 1400 heliostats, the maximum feed-water extraction from the boiler inlet can be reached, and excess solar energy is stored.

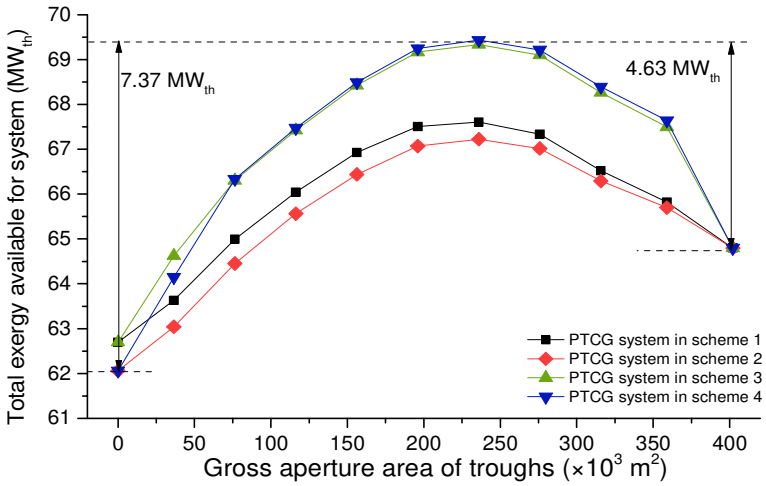

Figure 5. Total solar exergy available for the system

Figure 5 shows the total available solar exergy considering the energy to the TES when the maximum mass-flow of feed-water extraction is reached. From the figure, all four schemes can obtain a higher available solar exergy than SPCG or STCG system. The total available solar exergy is 62.70 MW_{th} in schemes 1 and 3, if all investments are used for the heliostat field, and 62.06 MW_{th} in schemes 2 and 4. For SPCG, the total solar exergy available is 64.80 MW_{th}. The maximum available solar exergy values are 67.61, 67.22, 69.33, and 69.43 MW_{th} in the four schemes, increased by 4.33-11.88% compared with that of the SPCG and STCG system. That is because, with a decrease in collectors and more heliostats configured, more solar exergy is introduced into the system due to the higher temperature of solar tower. As the heliostat field is enlarged, solar exergy introduced from the heliostats with the same investment gradually decreases due to the relatively lower efficiency of an increased number of heliostats. Ultimately, less solar exergy can be introduced from additional heliostats than from parabolic trough collectors with the same investment, which means the adding further heliostats is less cost-effective than adding parabolic trough area in this condition.

Therefore, PTCG can maintain a higher cost-efficiency of the solar field and obtain more solar exergy than SPCG and STCG systems.

Table 6. Comparison of this work and previous studies

	Power output (MW_e)	Investment for solar field (M$)	Solar exergy absorption limit (MW_{th})	Maximum solar exergy share (%)	Maximum available solar exergy (MW_{th})	Minimum coal consumption rate (g/kWh)	Studied or Novel
SPCG	660	68.27	80.88	7.89	64.80	253.17	Studied
STCG			55.93	6.81	62.70	255.83	Studied
PTCG			133.60	8.45	69.43	251.59	Novel

The comparison of the proposed PTCG and other solar-aided coal-fired systems in previous studies under the same investment condition are shown in Table 6. In PTCG, the amount of solar exergy absorption reaches an upper limitation only when the maximum extraction mass-flow from boiler inlet and feed-water preheaters are both reached. Therefore, the solar absorption limit is significantly improved in the proposed PTCG system. The solar exergy is also introduced more cost-effectively, with the maximum available solar exergy increased by 7.15-10.73%. With the same investment for solar field and the same electricity generation, the solar exergy share is increased by 0.56-1.64% in PTCG. As a result, the lowest coal consumption rate of 251.59 g/kWh can be obtained, reduced by at least 1.58 g/kWh and 4.24 g/kWh than that in SPCG and STCG systems, respectively. Therefore, the improved solar exergy contribution and better cost-effectiveness can be reached by a combination of solar energy at different temperatures in this novel PTCG system.

4.2.1 Effects of solar load on system performance

In this section, the effects of solar load are investigated. Figure 6 shows the change in coal consumption rate and available solar exergy for scheme1 and scheme 4 operating in different DNI conditions.

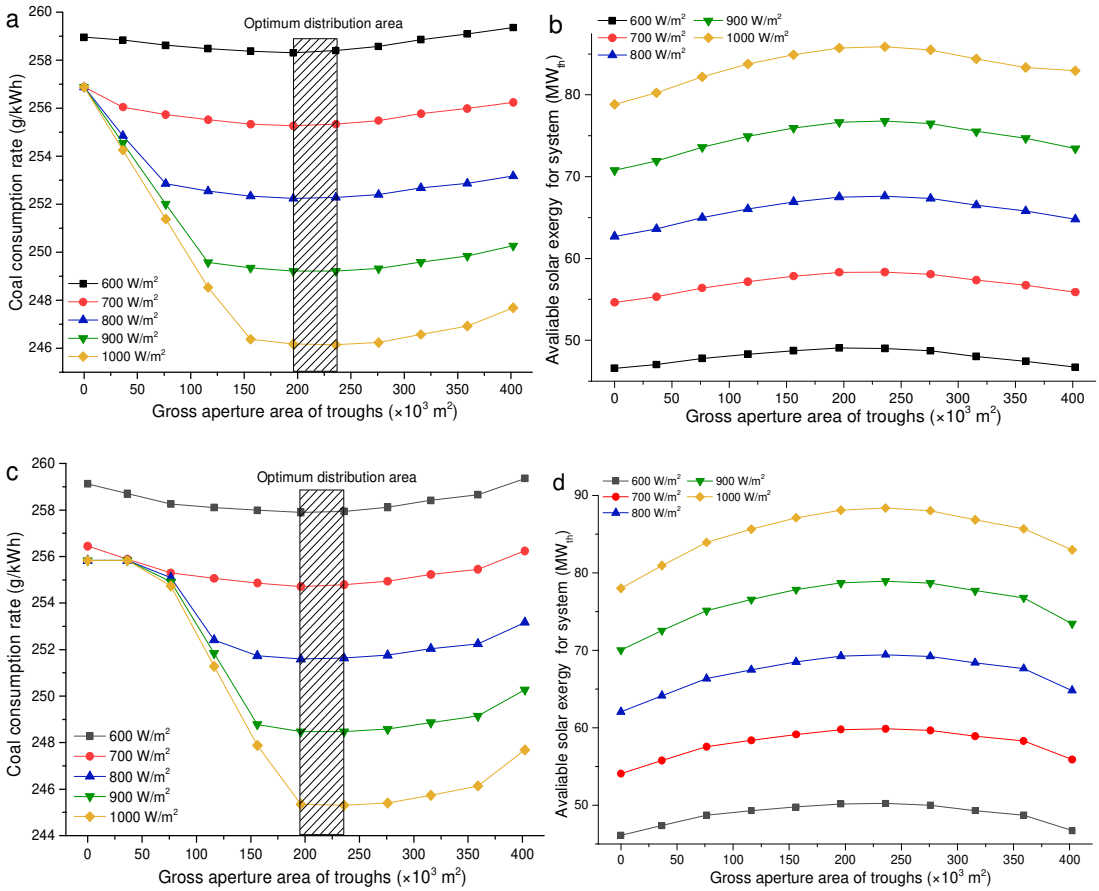

Figure 6. Effects of operating solar load on the plant performance, (a) coal consumption in scheme 1, (b) available solar exergy in scheme 1, (c) coal consumption in scheme 4, (d) available solar exergy in scheme 4

The two schemes are selected as examples because of the enhanced performances. From the figure, PTCG can obtain a lower coal consumption rate and higher available solar exergy than a SPCG and STCG in various operating solar load. Especially in high

DNI condition, the mass-flow of extraction restrain is easier to be reached in a SPCG and STCG, and the improvement in PTCG is more significant. As the DNI condition increases from 600 W/m^2 to 1000 W/m^2, the lowest coal consumption rates are 257.90, 254.71, 251.59, 248.46 and 245.31 g/kWh, obtained in scheme 4. Meanwhile, the maximum available solar exergy value increases from 50.23 to 88.36 MW_{th}. The available solar exergy is increased by 6.51%–13.28% compared with that of the SPCG and STCG systems, further saving 1.23–10.52 g/kWh coal consumption.

In different design DNI conditions, the required investment for the heliostat field will change due to the variation of the designed rated power of the tower and receiver. Figure 7 shows the change of coal consumption rate and available solar exergy in schemes 1 and 4 to explore the feasibility of PTCG system under different solar resources areas.

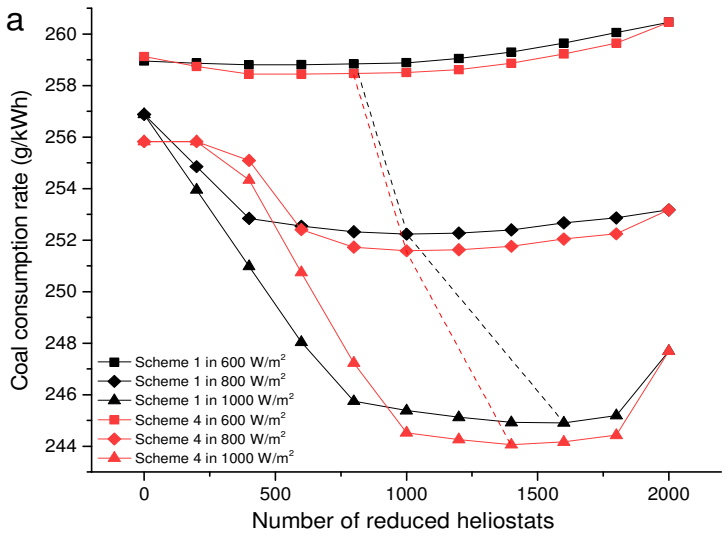

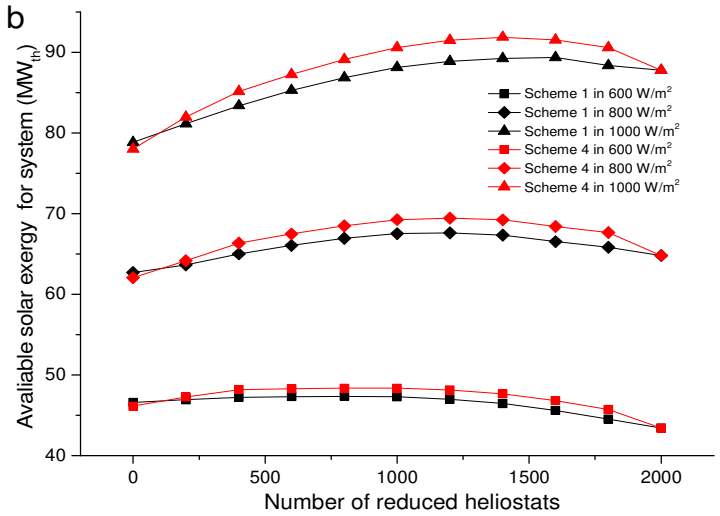

Figure 7. Effects of design DNI on plant performance with various investment distribution in scheme 1 and 4, (a) coal consumption rate, (b) total available solar exergy

In the 600 W/m^2 design condition, the lowest coal consumption rates in schemes 1 and 4 are 258.80 and 258.45 g/kWh, and the maximum available solar exergy values are 47.33 and 48.35 MW$_{th}$, respectively. The available solar exergy increased by 1.61%–11.40% compared with SPCG and STCG systems, further saving 0.15–2.02 g/kWh coal consumption. As the design DNI condition increases to 1000 W/m^2, the maximum available solar exergy reaches 89.36 and 91.88 MW$_{th}$, and the least coal consumption rates significantly decrease to 244.91 and 244.06 g/kWh, respectively, thus further saving 2.78–11.97 g/kWh of coal consumption. Therefore, the system performance improvement is more significant in area with abundant solar energy resources.

4.2.2 Effects of total solar field investment

The influence of total solar field investment is investigated in this section. With total solar field investments varies in the range of 48.60 M$ to 87.41 M$, which is can be used for a maximum 1400 to 2600 heliostats, figures 8 shows the change in coal

consumption rate and available solar exergy in schemes 1 and 4.

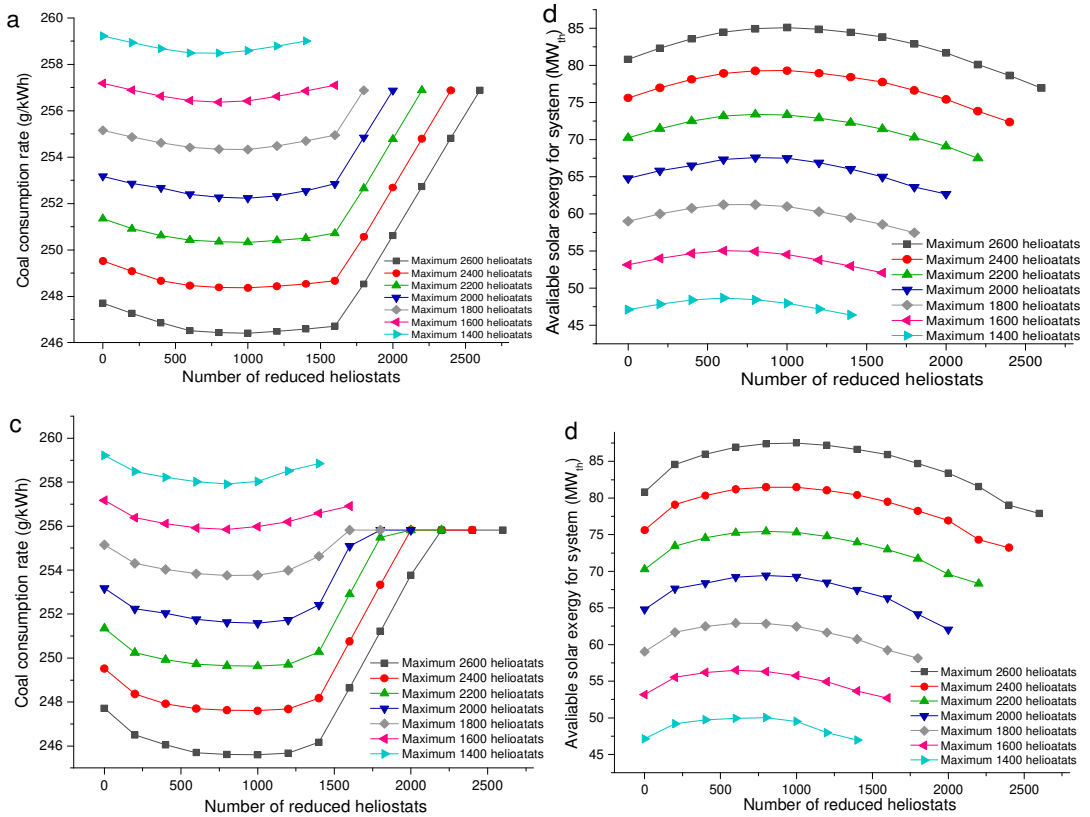

Figure 8. Effects of total solar field investment on the plant performance under different investment distribution, (a) coal consumption in scheme 1, (b) available solar exergy in scheme 1, (c) coal consumption in scheme 4, (d) available solar exergy in scheme 4

The coal consumption rate and available solar exergy changes similarly in two schemes in different solar field distributions as the total investment for the solar field increases. In scheme 1, the least coal consumption rate decreases from 258.48 g/kWh to 246.41 g/kWh, and the maximum available solar exergy increases from 48.69 MW_{th} to 85.10 MW_{th}. In scheme 4, the maximum mass-flow of feed-water extraction from the boiler inlet is reached in systems with more than 1400 heliostats, and the coal consumption rate is restricted. The least coal consumption rate decreases from 257.91 g/kWh to 245.60 g/kWh, further declining by 1.31–2.11 g/kWh compared with that in

the SPCG system. The available solar exergy increases from 50.05 MW_{th} to 87.51 MW_{th}, which is 2.92%–12.35% higher than that in the SPCG and STCG systems.

4.2.4 Effects of unit solar field cost

Figures 9 shows the effects of unit collector cost on coal consumption rate and available solar exergy for systems in schemes 1 and 4, which varies between 140 \$/m^2 and 180 \$/m^2.

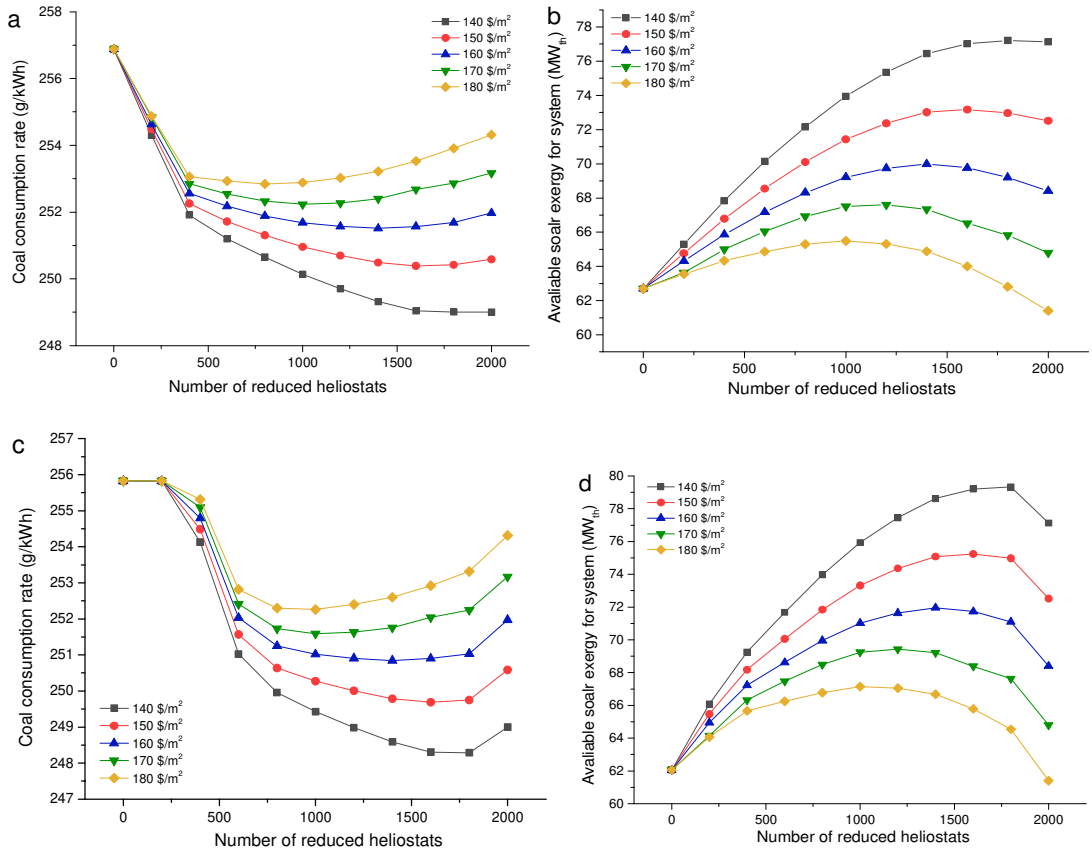

Figure 9. Effects of unit trough cost on the plant performance with the same total investment under different distribution, (a) coal consumption in scheme 1, (b) available solar exergy in scheme 1, (c) coal consumption in scheme 4, (d) available solar exergy in scheme 4

In the SPCG system, the coal consumption rate decreases from 254.32 g/kWh to 249.00 g/kWh as the unit collector cost decreases from 180 \$/m^2 to 140 \$/m^2, and available solar exergy increases from 61.41 MW_{th} to 77.13 MW_{th}. In scheme 1, when

the unit collector cost decreases to 140 \$/m^2, the least coal consumption rate is obtained in the SPCG system. In scheme 4, the least coal consumption rates are 252.26, 251.59, 250.84, 249.69, and 248.29 g/kWh. Accordingly, 0.71–2.06 g/kWh coal fuel can be further saved compared with that of the SPCG system, but the gap between the two systems narrowed as unit collector cost decreased. Therefore, PTCG can obtain a better performance compared with the SPCG and STCG systems within a wide range considering the variety of collector and heliostat unit cost.

5 Conclusions

In this study, the PTCG system is proposed, and the performances in four schemes with different distributions between troughs and heliostat field are studied and compared. The conclusions are summarised as follow:

(1) The improved solar exergy contribution and better cost-effectiveness can be reached by a combination of solar energy at different temperatures in this novel PTCG system. All four schemes in PTCG can reach a lower coal consumption rate and higher available solar exergy than SPCG and STCG because of improved solar contribution limitation and higher cost-efficiency. In scheme 4, the lowest coal consumption rate is 251.59 g/kWh, and the maximum available solar exergy is 69.43 MW_{th}. Accordingly, available solar exergy increases by 7.83%–11.88% and 1.58–4.24 g/kWh coal fuel can be further saved than SPCG and STCG.

(2) Enhanced performance can be obtained in PTCG in various solar load

conditions. The improvement is more significant in high DNI condition due to the easily reached extraction mass-flow limitation in other systems. As the operating DNI condition increases from 600 W/m^2 to 1000 W/m^2, the maximum available solar exergy increased from 50.23 MW_{th} to 88.36 MW_{th} and 1.23–10.52 g/kWh coal consumption can be further saved compared with the SPCG and STCG.

(3) Superior performance can be obtained in the proposed system in various total solar field investment conditions. As the total solar field investment varies in the range of from 48.60 M$ to 87.41 M$, the least coal consumption rate decreases from 257.91 g/kWh to 245.60 g/kWh, further decreasing by 1.31–2.11 g/kWh compared with that in the SPCG system.

(4) PTCG can obtain a better performance within a wide range considering the variety of collector unit. However, the difference gap is narrowed as unit collector cost decreases. As unit collector cost decreases from 180 to 140 \$/m^2, 0.71–2.06 g/kWh coal fuel can be further saved in the proposed system in scheme 4 compared with the SPCG.

Acknowledgements

The research work is supported by China National Natural Science Foundation (No. 51776063), Science Fund for Creative Research Groups of the National Natural Science Foundation of China (No. 51821004), the Fundamental Research Funds for the Central Universities (2019QN010) and China Scholarship Council.

References

[1] Panwar NL, Kaushik SC, Kothari S. Role of renewable energy sources in environmental protection: A review. Renewable and Sustainable Energy Reviews. 2011;15:1513-24.

[2] Bp G. Bp Statistical Review of World Energy. 2018. https://www. bp. com/en/global/corporate/energy-economics/statistical-review-of-world-energy. html (accessed on 4 September 2018). Sustainability, 2018, 10(3195): 17.

[3] Zhao X, Yin H, Zhao Y. Impact of environmental regulations on the efficiency and CO2 emissions of power plants in China. Applied Energy. 2015;149:238-47.

[4] Forrester J. The Value of CSP with Thermal Energy Storage in Providing Grid Stability. Energy Procedia. 2014;49:1632-41.

[5] Zoschak RJ, Wu SF. Studies of the direct input of solar energy to a fossil-fueled central station steam power plant. Sol Energy 1975;17(5):297e305.

[6] Hu E, Yang Y, Nishimura A, Yilmaz F, Kouzani A. Solar thermal aided power generation. Applied Energy. 2010;87:2881-5.

[7] Yan Q, Yang Y, Nishimura A, Kouzani A, Hu E. Multi-point and Multi-level Solar Integration into a Conventional Coal-Fired Power Plant†. Energy & Fuels. 2010;24:3733-8.

[8] Yang Y, Yan Q, Zhai R, Kouzani A, Hu E. An efficient way to use medium-or-low temperature solar heat for power generation – integration into conventional power plant. Applied Thermal Engineering. 2011;31:157-62.

[9] Yan Q, Hu E, Yang Y, Zhai R. Dynamic modeling and simulation of a solar direct steam-generating system. International Journal of Energy Research. 2010;34:1341-55.

[10] Rech S, Lazzaretto A, Grigolon E. Optimum integration of concentrating solar technologies in a real coal-fired power plant for fuel saving. Energy Conversion and Management. 2018;178:299-310.

[11] Qin J, Hu E, Nathan GJ. The performance of a Solar Aided Power Generation plant with diverse "configuration-operation" combinations. Energy Conversion and Management. 2016;124:155-67.

[12] Li J, Wu Z, Zeng K, Flamant G, Ding A, Wang J. Safety and efficiency assessment of a solar-aided coal-fired power plant. Energy Conversion and Management. 2017;150:714-24.

[13] Junjie W, Hongjuan H, Yongping Y. Research on the Performance of Coal-fired Power System Integrated with Solar Energy. Energy Procedia. 2014;61:791-4.

[14] Wu J, Hou H, Yang Y. The optimization of integration modes in solar aided power generation (SPCG) system. Energy Conversion and Management. 2016;126:774-89.

[15] Wu J, Hou H, Yang Y, Hu E. Annual performance of a solar aided coal-fired power generation system (SACPG) with various solar field areas and thermal energy storage capacity. Applied Energy. 2015;157:123-33.

[16] Wu J, Hou H, Yang Y. Annual economic performance of a solar-aided 600 MW coal-fired power generation system under different tracking modes, aperture areas, and storage capacities. Applied Thermal Engineering. 2016;104:319-32.

[17] Hong-juan H, Zhen-yue Y, Yong-ping Y, Si C, Na L, Junjie W. Performance evaluation of solar aided feedwater heating of coal-fired power generation (SAFHCPG) system under different operating conditions. Applied Energy. 2013;112:710-8.

[18] Peng S, Hong H, Wang Y, Wang Z, Jin H. Off-design thermodynamic performances on typical days of a 330MW solar aided coal-fired power plant in China. Applied Energy. 2014;130:500-9.

[19] Zhang N, Hou H, Yu G, Hu E, Duan L, Zhao J. Simulated performance analysis of a solar aided power generation plant in fuel saving operation mode. Energy. 2019;166:918-28.

[20] Wang J, Duan L, Yang Y, Yang Z, Yang L. Study on the general system integration optimization method of the solar aided coal-fired power generation system. Energy. 2019;169:660-73.

[21] Wang J, Duan L, Yang Y, Pang L, Yang L. Multi-objective optimization of solar-aided coal-fired power generation system under off-design work conditions. Energy Science & Engineering. 2019;7:379-98.

[22] Feng L, Liao H, Wang P, Huang J, Schumacher KL. A technique to avoid two-phase flow in solar collector tubes of the direct steam generation system for a solar aided power generation plant. Applied Thermal Engineering. 2019;148:568-77.

[23] Huang C, Hou H, Hu E, Yu G, Peng H, Yang Y, et al. Performance maximization of a solar aided power generation (SAPG) plant with a direct air-cooled condenser in power-boosting mode. Energy. 2019;175:891-9.

[24] Huang C, Hou H, Hu E, Yu G, Peng H, Zhao J, et al. Stabilizing operation of a solar aided power generation (SAPG) plant by adjusting the burners' tilt and attemperation flows in the boiler. Energy. 2019;173:1208-20.

[25] Zhai R, Peng P, Yang Y, Zhao M. Optimization study of integration strategies in solar aided coal-fired power generation system. Renewable Energy. 2014;68:80-6.

[26] Zhai R, Liu H, Li C, Zhao M, Yang Y. Analysis of a solar-aided coal-fired power generation system based on thermo-economic structural theory. Energy. 2016;102:375-87.

[27] Zhu Y, Zhai R, Zhao M, Yang Y, Yan Q. Evaluation methods of solar contribution in solar aided coal-fired power generation system. Energy Conversion and Management. 2015;102:209-16.

[28] Suresh MVJJ, Reddy KS, Kolar AK. 4-E (Energy, Exergy, Environment, and Economic) analysis of solar thermal aided coal-fired power plants. Energy for Sustainable Development. 2010;14:267-79.

[29] Pierce W, Gauché P, von Backström T, Brent AC, Tadros A. A comparison of solar aided power generation (SPCG) and stand-alone concentrating solar power (CSP): A South African case study. Applied Thermal Engineering. 2013;61:657-62.

[30] Jamel MS, Abd Rahman A, Shamsuddin AH. Advances in the integration of solar thermal energy with conventional and non-conventional power plants. Renewable and Sustainable Energy Reviews. 2013;20:71-81.

[31] Zhu Y, Zhai R, Peng H, Yang Y. Exergy destruction analysis of solar tower aided

coal-fired power generation system using exergy and advanced exergetic methods. Applied Thermal Engineering. 2016;108:339-46.

[32] Zhu Y, Zhai R, Qi J, Yang Y, Reyes-Belmonte MA, Romero M, et al. Annual performance of solar tower aided coal-fired power generation system. Energy. 2017;119:662-74.

[33] Zhu Y, Zhai R, Yang Y, Reyes-Belmonte M. Techno-Economic Analysis of Solar Tower Aided Coal-Fired Power Generation System. Energies. 2017;10:1392.

[34] Zhang M, Du X, Pang L, Xu C, Yang L. Performance of double source boiler with coal-fired and solar power tower heat for supercritical power generating unit. Energy. 2016;104:64-75.

[35] Zhang M, Xu C, Du X, Amjad M, Wen D. Off-design performance of concentrated solar heat and coal double-source boiler power generation with thermocline energy storage. Applied Energy. 2017;189:697-710.

[36] Li C, Zhai R, Yang Y, Patchigolla K, Oakey JE. Thermal performance of different integration schemes for a solar tower aided coal-fired power system. Energy Conversion and Management. 2018;171:1237-45.

[37] Li C, Yang Z, Zhai R, Yang Y, Patchigolla K, Oakey JE. Off-design thermodynamic performances of a solar tower aided coal-fired power plant for different solar multiples with thermal energy storage. Energy. 2018;163:956-68.

[38] Li C, Zhai R, Yang Y, Patchigolla K, Oakey JE, Turner P. Annual performance analysis and optimization of a solar tower aided coal-fired power plant. Applied Energy.

2019;237:440-56.

[39] Weather Data of System Advisor Model, https://sam.nrel.gov/weather/; [accessed 17.08.28].

[40] Zhai R, Liu H, Chen Y, Wu H, Yang Y. The daily and annual technical-economic analysis of the thermal storage PV-CSP system in two dispatch strategies. Energy Conversion and Management. 2017;154:56-67.

[41] Liu H, Zhai R, Fu J, Wang Y, Yang Y. Optimization study of thermal-storage PV-CSP integrated system based on GA-PSO algorithm. Solar Energy, 2019, 184: 391-409.

[42] Turchi C S, Heath G A. Molten salt power tower cost model for the system advisor model (SAM). National Renewable Energy Lab.(NREL), Golden, CO (United States), 2013.

[43] Kurup P, Turchi C S. Parabolic trough collector cost update for the system advisor model (SAM). National Renewable Energy Laboratory, Golden, CO, Technical Report No. NREL/TP-6A20-65228. https://www. nrel. gov/docs/fy16osti/65228. pdf, 2015.